International Nano Letters (2018) 8:31–39
https://doi.org/10.1007/s40089-018-0230-x

ORIGINAL ARTICLE

Heterogeneous photocatalytic degradation of toluene in static environment employing thin films of nitrogen-doped nano-titanium dioxide

Yasun Y. Kannangara[1,2] · Ruchira Wijesena[1] · R. M. G. Rajapakse[2,3] · K. M. Nalin de Silva[1,4]

Received: 18 August 2017 / Accepted: 26 March 2018 / Published online: 17 April 2018

Abstract
Photocatalytic semiconductor thin films have the ability to degrade volatile organic compounds (VOCs) causing numerous health problems. The group of VOCs called "BTEX" is abundant in houses and indoor of automobiles. Anatase phase of TiO_2 has a band gap of 3.2 eV and UV radiation is required for photogeneration of electrons and holes in TiO_2 particles. This band gap can be decreased significantly when TiO_2 is doped with nitrogen (N-TiO_2). Dopants like Pd, Cd, and Ag are hazardous to human health but N-doped TiO_2 can be used in indoor pollutant remediation. In this research, N-doped TiO_2 nano-powder was prepared and characterized using various analytical techniques. N-TiO_2 was made in sol–gel method and triethylamine ($N(CH_2CH_3)_3$) was used as the N-precursor. Modified quartz cell was used to measure the photocatalytic degradation of toluene. N-doped TiO_2 nano-powder was illuminated with visible light (xenon lamp 200 W, $\lambda = 330$–800 nm, intensity = 1 Sun) to cause the degradation of VOCs present in static air. Photocatalyst was coated on a thin glass plate, using the doctor-blade method, was inserted into a quartz cell containing 2.00 µL of toluene and 35 min was allowed for evaporation/condensation equilibrium and then illuminated for 2 h. Remarkably, the highest value of efficiency 85% was observed in the 1 µm thick N-TiO_2 thin film. The kinetics of photocatalytic degradation of toluene by N-TiO_2 and P25-TiO_2 has been compared. Surface topology was studied by varying the thickness of the N-TiO_2 thin films. The surface nanostructures were analysed and studied with atomic force microscopy with various thin film thicknesses.

Keywords N-doped TiO_2 · Photocatalytic thin film · Volatile organic compounds · Surface study

Introduction

Titanium dioxide (TiO_2) has been known as one of the most popular photocatalytic semiconductor materials [1–3] and has attracted a great deal of attention because of its good stability [4, 5], nontoxicity [6], high photocatalytic efficiency [7] and low cost [8, 9]. However, TiO_2 has a high band gap ($E_g = 1$ eV) in its anatase phase [10] and, as a result, it can only absorb radiation in the UV range. This phenomenon limits its practical ability to use as solar energy-driven photocatalyst since the solar radiation has only about 5% of UV radiation. To overcome this barrier of higher band gap, several modifications have been proposed. Doping TiO_2 with other materials, such as non-metals [11, 12] and metals [13, 14], has been investigated for extending the radiation absorption of TiO_2 to the visible range to maximize the use of the visible light region of solar spectrum. In the past few decades, considerable research studies have shown that doping TiO_2 with non-metal elements, such as carbon, boron,

✉ K. M. Nalin de Silva
kmnd@chem.cmb.ac.lk

Yasun Y. Kannangara
yasunyk@gmail.com

Ruchira Wijesena
ruchiraw@slintec.lk

R. M. G. Rajapakse
rmgr@pdn.ac.lk

[1] Sri Lanka Institute of Nanotechnology (SLINTEC), Nanotechnology and Science Park, Mahenwatte, Pitipana, Homagama, Sri Lanka

[2] Postgraduate Institute of Science, University of Peradeniya, Peradeniya, Sri Lanka

[3] Department of Chemistry, University of Peradeniya, Peradeniya, Sri Lanka

[4] Department of Chemistry, Faculty of Science, University of Colombo, Colombo 00300, Sri Lanka

fluorine, nitrogen and sulphur, enables the realization of visible light-responsive TiO_2. Among those studies, nitrogen doping has been proved to be a modest and most effective technique [15] to achieve visible light stimulated photocatalytic activities of TiO_2. However, most of the studies on nitrogen-doped TiO_2 have assumed that the nitrogen doping results in a surface or sub-surface modification making it difficult to narrow down the band gap in the bulk of TiO_2. Such a surface modification could only improve the visible light absorption in the range of 400–600 nm. These materials have been used in different forms, such as aqueous TiO_2 suspensions [16], thin films [17] and nanocoatings in different practical applications. Thin films can be easily fabricated using the sol–gel method, dip-coating and by spin-coating techniques which constitute one of the simplest and promising approaches for synthesizing thin film materials with controlled optical, structural and morphological properties. These films have been found to be attractive in heterogeneous photocatalytic degradation (HPD) of volatile organic compounds [18, 19].

The present study investigates the use of nitrogen-doped TiO_2 thin films fabricated by sol–gel method, followed by doctor blading on glass surfaces and subsequent annealing to use in the photocatalytic degradation of VOC compounds in indoor environments. Effect of layer thickness on the degradation effect will also be described. Thin film formation method is very important to maintain right porosity and the required surface roughness for efficient degradation of VOC compounds.

Experimental

Material

P25-TiO_2 (Sigma-Aldrich, Germany), $AgNO_3$ (> 99% (Titration) Sigma-Aldrich, Germany) and triethylamine ($N(CH_2CH_3)_3$/Et_3N) (Sigma-Aldrich, Germany), tetrabutyltitanate [$Ti(OC_4H_9)_4$, Sigma-Aldrich, Germany], isopropyl alcohol (C_3H_7OH), conc. HNO_3 and conc. acetic acid (CH_3COOH) (Sigma-Aldrich, Germany) were used as received.

Preparation of N-TiO_2 nanoparticles

The N-TiO_2 was prepared by the sol–gel method [20, 21] and it was done by following a procedure reported by Wu et al. [22] where isopropyl alcohol (C_3H_7OH) and $Ti(OC_4H_9)_4$, in acidic medium, were used to prepare TiO_2 nanoparticles. 5.0 mL of C_3H_7OH and $Ti(OC_4H_9)_4$ was mixed with 30.0 mL of 0.20 mol dm^{-3} HNO_3 solution. Then, the mixture was aged for 12 h to obtain a transparent nanosol. 2.0 mL of $N(CH_2CH_3)_3$ was added and well mixed and allowed to age for 12 h, with stirring, at ambient temperature. Then, the sol was refluxed, at 100 °C, for 6 h. Continuous stirring was always maintained to prevent the sol from coagulation. Finally, the sol was dried at 120 °C for 6 h and then calcined at 450 °C for 4 h. During the calcination process, sample turned to a light yellowish colour.

Characterization of the N-TiO_2 nanoparticles

The N-TiO_2 was examined by scanning electron microscopy (SEM) HITACHI-SU 6600 Analytical Variable Pressure FE-SEM with gold ion sputter, E-1020 microscope, operated at 20 kV in the secondary electron mode. X-ray diffraction (XRD) patterns were collected on Bruker D8 Focus X-ray Powder Diffractometer operated at 40 kV and 40 mA, using Cu K_α radiation ($\lambda = 0.15418$ nm) in the thin film mode with a step size of 0.2° and counting time of 1.0 s per step. UV–Vis–NIR spectrophotometer (*UV 3600, Shimadzu, Japan*) was used to determine band gaps of semiconductors using diffuse reflectance mode, using $BaSO_4$ as reflectance sample, and the kinetics of photodegradation was evaluated in the absorbance mode, with air as the reference. Reflectance spectra were analysed at ambient conditions, in the wavelength range of 200–600 nm. Surface topology and surface roughness of the thin films were obtained by Atomic Force Microscopy (AFM) from Park Systems XE-100 in the non-contact mode, with cantilever tip of 2.8 µm thickness and less than 10 nm tip radius. Light source used was a xenon lamp (200 W) from the solar simulator (US-900) with the intensity of light of 1 Sun (AM 1.5) in the wavelength (λ) range from 330 to 800 nm.

Thin film preparation

0.0500 g of N-TiO_2 nano-powder was measured using a microbalance (KERN ALN 120-4n) and mixed with 2 mL of 2% CH_3COOH solution and ground for 20 min. One drop of Triton-X-100 was added and the mixture was again ground continuously using an agate mortar and pestle. The mixture turned to a slurry paste and this nanosol was ground for another 10 min, until it was ready to cast on the glass slides. It was then pasted on a 1 cm^2 area of a glass slide using the doctor blade method [23, 24]. After the thin films was dried, it was sintered, at 450 °C, for 30 min, using a muffle furnace (Norbertherm-B 180) to remove any organic materials present in the TiO_2 nanoparticles and to have an interconnected matrix of nanoparticles.

Photocatalytic activity

The photocatalytic activities of these semiconductor thin films were determined by measuring the degradation of toluene vapour under illumination using the solar simulator

(*US-900*) with 1 Sun intensity in the wavelength (λ) range in 330–800 nm. The photocatalyst (0.213 g per each plate) was coated on a (1 cm^2) thin glass plate using the doctor-blade method. The initial volume of toluene added to the modified quartz cell was 2.00 µL. For control test, first, P25-TiO_2 thin film was exposed to toluene vapour in the modified quartz cell and the reaction was carried out in the dark. Then, in the HPD step, P25-TiO_2 thin film was placed as same as in control step. The P25-TiO_2 thin film was exposed to the visible light under identical way. At given time intervals of illumination (5 min per each time interval), the toluene concentration was analysed by a UV–Vis spectrophotometer (*UV-3600, Shimadzu, Japan*). When measuring the kinetics of the toluene degradation by N-TiO_2 thin films, the same procedure was followed. The degradation efficiency was calculated using Eq. (1).

$$\eta(\%) = \frac{C_0 - C_1}{C_0} \times 100\% \quad (1)$$

The degradation kinetics was measured at static conditions which is prevailing in indoor air. All the experiment trials of VOC degradations were measured with constant volume of 2 µL $C_6H_5CH_3$ and their reaction rates have kept fixed by keeping the constant initial concentration of toluene vapour. The degradation rate was taken as C/C_0, where C_0 is the initial concentration and C is the concentration at a given time, and its variation with time is shown in Fig. 4. Here, the quartz cell covered plastic top also might absorb some amount of $C_6H_5CH_3$ and to prevent this unnecessary absorption; ultrathin aluminium foil was used to cover the plastic top.

Roughness analysis

We reported three main standard statistical parameters to describe the nanostructure of thin film surface: average roughness (R_a), root mean squared roughness (R_q) and skewness (R_{sk}) [25]. For topographical analysis, these parameters were commonly used for understanding the roughness measurements, as well as overall description of the nanoarchitecture of the thin films presented. The degradation rate of toluene vapour has been studied with different thicknesses. A set of experiments using different weighted thin films of N-TiO_2 from 0.71 to 5.00 mg was carried out with initial amount of toluene 2 µL for irradiation of 2 h. Atomic Force Microscope (AFM) from Park Systems XE-100 was used to scan the surface topology of each N-TiO_2 thin films. The amplitude parameters are the principal parameters in characterizing the surface topography. The average roughness (R_a) and the root mean square roughness (R_q) which were monitored described the surface architecture in vertical dimensions quite well, but offer no insight into the horizontal dimensions of the surface. Skewness (R_{sk}) which gives more descriptive information in horizontal dimensions about the surface structure was also evaluated.

Results and discussion

PXRD characterization

Powder X-ray diffractogram of the TiO_2 thin film is shown in Fig. 1. TiO_2 primarily exists in different phases: anatase and rutile with different band gap values of 3.2 and 3.0 eV, respectively, are the commonest.

P25 is known to have combination of anatase and rutile phases [26] which are in the positions (101, 110, 112, 200

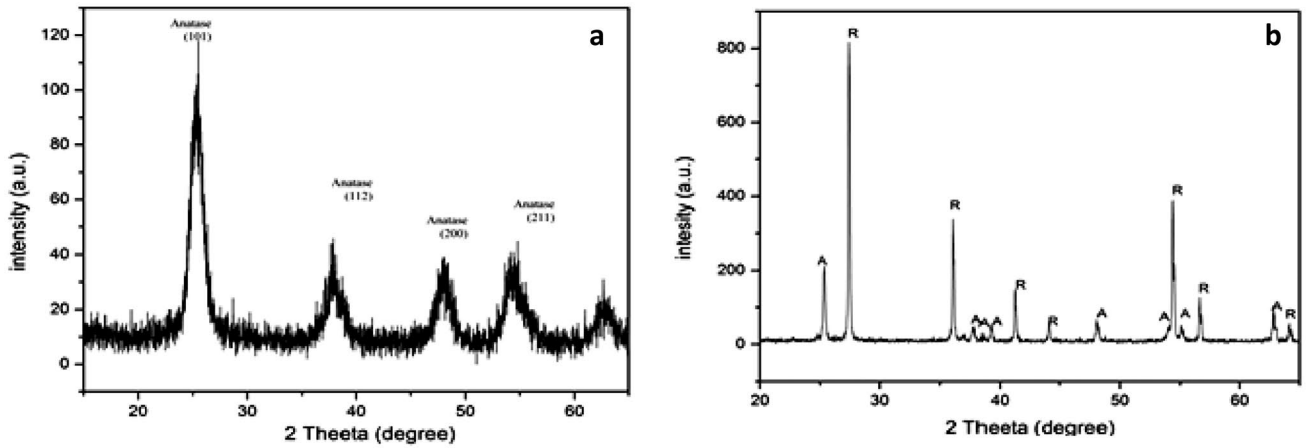

Fig. 1 Powder X-ray diffraction patterns of **a** N-doped TiO_2 nanoparticles and **b** P25 TiO_2 nanoparticles (commercial)

and 211) though N-doped TiO_2 shows crystallographic peaks that corresponds only to anatase crystal structure. These Miller Indices are located in 101, 112, 200 and 211 at 2θ values of: 25.38°, 38.14°, 48.04° and 55.02°, respectively [27]. Mean crystallite size, as analysed by Debye–Scherrer equation, is 55 nm.

UV–visible characterization

According to the Fig. 2, the band gap energy of N-TiO_2 had been calculated using the Planck's energy equation [28]. A band gap ~ 3.00 eV which is related to the cut-off wavelength of 410.3 nm is obtained for N-doped TiO_2 nanomaterial. Initially, the white powder P25-TiO_2 turned yellow after the $N(CH_2CH_3)_3$ treatment and annealing. N-TiO_2 displayed a strong absorption band at 410.3 nm, which can be attributed to the doped nitrogen in the anatase structure. According to *Lynch* et al. [29] doping atoms can be attached to TiO_2 matrix in the substitutional and interstitial modes. Kubelka–Munk transformation provides a conversion of reflectance to Kubelka–Munk (KM) [30] units that, under certain circumstances, is directly proportional to the absorbance. The absorption spectrum shows the band gap energy (Fig. 2) by giving the cutoff wavelength ~ 410 nm and showing that N-TiO_2 band gap has decreased and hence it can be excited by visible light irradiation for use in photocatalytic degradation processes.

The SEM images of N-TiO_2 nanomaterial at three different magnifications are shown in Fig. 3. Figure 3a shows the N-TiO_2 nanomaterial having the majority of spherical granules with average particle size of 40 nm. Nanoparticles which have irregular shapes are scattered on the surface. Powders are smaller aggregated particles, resulting in a high porous volume. Figure 3d shows the cross-sectional image of the glass substrate and the thin film at 1000 magnification.

Kinetic analysis

In Fig. 4, line (a) in both graphs a and b, there is a slight reduction of amount of toluene with time. This might be due to the absorption of $C_6H_5CH_3$ by thin film's nanomaterial or may also be due to leakages or may be due to both. Line (a) in both graphs was taken as control. The reaction under visible light illumination (line: b in Fig. 4a) shows increased reduction of toluene vapour with time, representing photocatalytic degradation in addition to leakages and adsorptions. The difference of (a) and (b) shows the reduction of toluene by photocatalytic degradation. The HPD of toluene on the N-TiO_2 thin film follows three main stages: (1) the adsorption of $C_6H_5CH_3$ molecules on to the surface of thin coating of N-TiO_2; (2) formation of $OH^{\bullet}$, $O_2^{\bullet}$, $HOO^{\bullet}$ and $^{\bullet}OH$ which are generally called reactive oxidizing species (ROSs) due to the reaction of electrons in the CB of N-TiO_2 with O_2 in air (3) reactions of these ROSs with toluene and also oxidation of toluene by the holes in the valence band of N-TiO_2.

According to the Fig. 4, 10% of toluene has degraded by P25-TiO_2 thin film during 185 min. In contrast, 45% degradation of toluene has taken place by N-TiO_2 thin film, during 110 min showing the effectiveness of toluene oxidation by N-TiO_2 when compared to that by P-25.

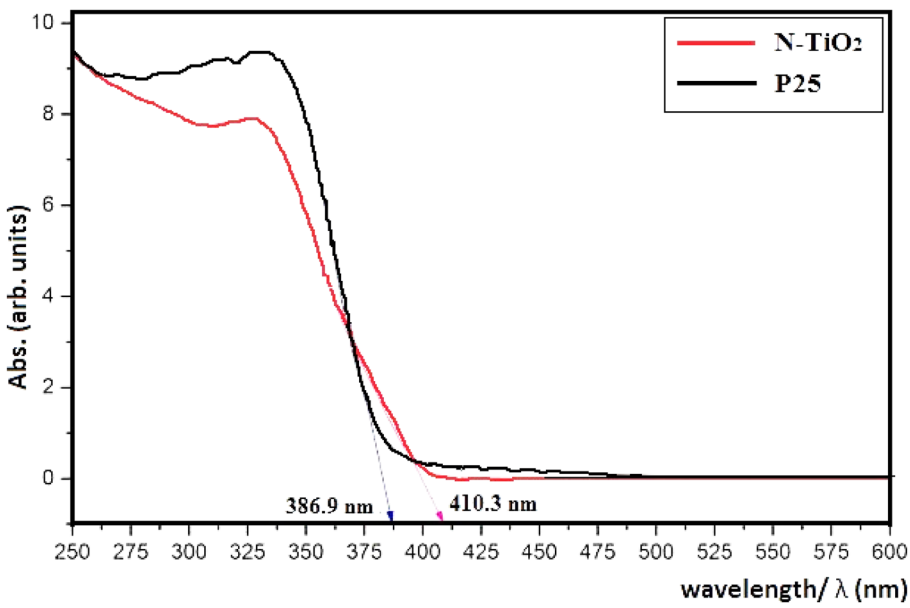

Fig. 2 UV–Visible diffuse reflectance measurement of N-doped TiO_2

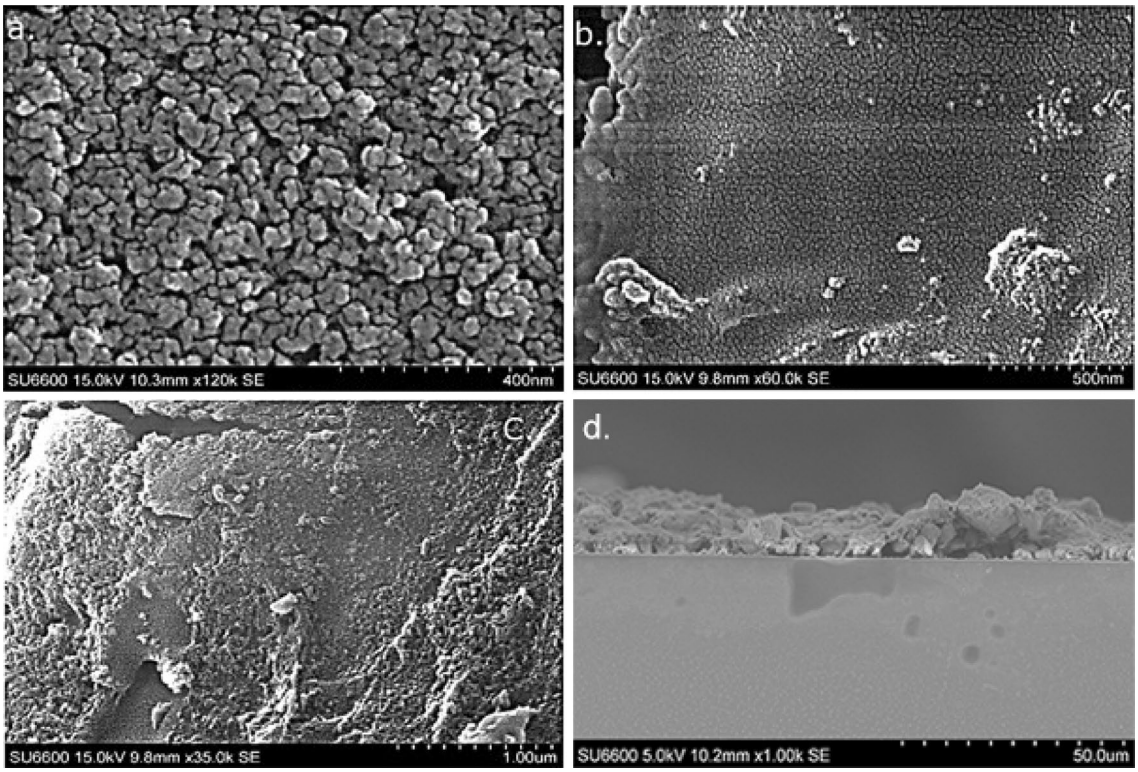

Fig. 3 Scanning electron microscopic images of N-TiO_2 thin films under different magnifications; **a** ×120,000, **b** ×60,000, **c** ×35,000 and **d** cross sectional image of the glass substrate and the thin film at ×1000 magnification

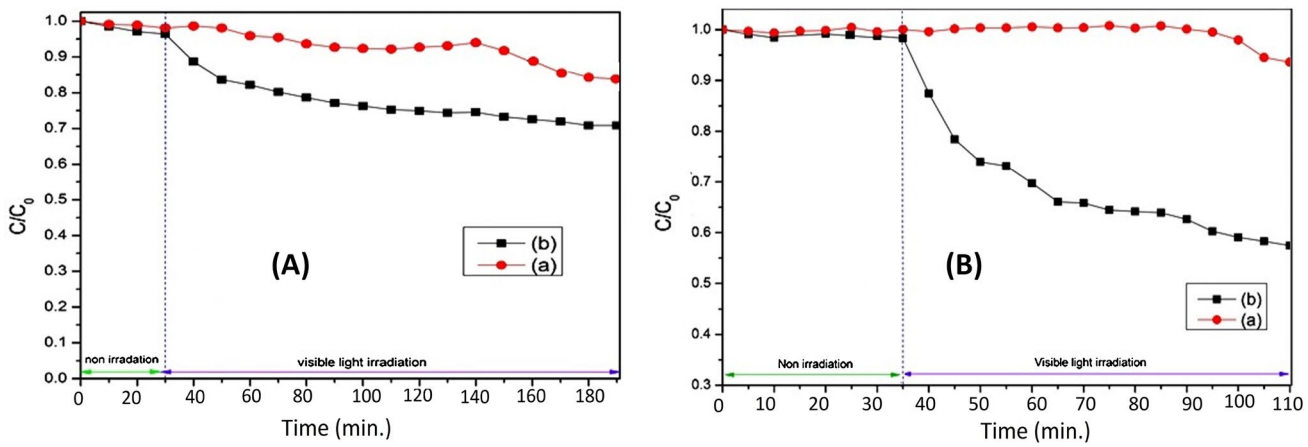

Fig. 4 Toluene degradation by P25 TiO_2 (**a**) and **b** N-TiO_2 respectively **a** in the absence of and **b** under illumination of visible light

Effect of the roughness to the heterogeneous photocatalytic degradation (HPD) efficiency

The Photocatalytic degradation rate of toluene vapour has been studied with different thicknesses of photocatalytic films and the results are depicted in Fig. 5. The degradation rates of toluene for different amounts of N-TiO_2 show that photocatalytic degradation efficiency improved systematically with the amount of N-TiO_2 when the amount of N-TiO_2 in the film is varied from 0.71 to 5.00 mg. When increasing the amount of N-TiO_2 further, the degradation efficiency has also increased but after some optimum thickness, the efficiency decreased, as revealed by the results shown in Table 1. The thickness of the film

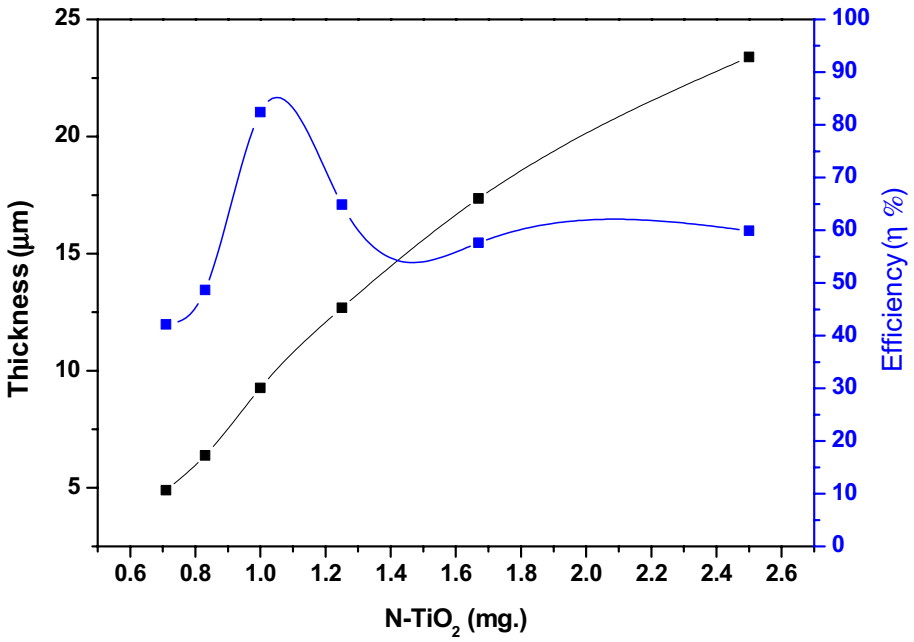

Fig. 5 **a** Effect of N-TiO_2 amount on thin films for toluene vapour degradation and **b** effect of N-TiO_2 thickness on thin films of toluene vapour degradation

Table 1 Information of thickness and efficiency of N-TiO_2 thin films

Sample name	N-TiO_2 amount (mg)	Thickness (μm)	Efficiency/η (%)
a	0.71	4.89	42.10
b	0.83	6.38	48.63
c	1.00	9.26	82.39
d	1.25	12.69	64.83
e	1.67	17.35	57.63
f	2.50	23.40	59.91
g	5.00	30.21	39.98

containing 1.00 mg of N-TiO_2 is 9.26 μm thickness and it shows the optimum best efficiency of 82.39%.

The film: *g* containing 5.00 mg of N-TiO_2 shows the lowest efficiency when compared to the other films. It also reveals that the efficiency increases when the amount of N-TiO_2 in the film is deceased from 5.00 to 1.00 mg. It is possible that when the film is too thick, its particles on the surface get flocculated and agglomerated, thus preventing the penetration of the light into the film. It is likely that the higher the thickness of the layer the more the particles in the film and hence higher is the particle aggregation. As such, the optimum thickness to give high efficiency is the 9.26 μm which has 1.00 mg of N-TiO_2 in the film.

The atomic force microscopic images of N-TiO_2 photocatalytic thin films with different thicknesses are shown in Fig. 6. The efficiency has shown significant variation with nano-scale roughness of N-TiO_2 thin film and the thin film which has minimum R_a (average roughness) value shows the highest efficiency (η %) value but other factors such as root mean square (RMS) roughness R_q and R_{sk} (skewness) have also effected. When R_a values decline, the granules in the surface become smaller and the surface area is significantly increased. R_a and R_q values are amplitude parameters and are the principle parameters in characterizing the surface topography. Another important functional or statistical parameter is called the skewness (R_{sk}) which gives information about the surface structure. R_{sk} is used to measure the profile symmetry about mean line. Zero R_{sk} indicates the highest symmetrical height distribution. In general, if the height distribution is asymmetrical, and the surface has more peaks than valleys, the skewness moment is positive and if the surface is more planar and valleys are predominant the skewness is negative.

The R_a, R_q and R_{sk} factors of samples *a*–*g* are illustrated in Fig. 7. The highest HPD efficiency (η %) was found in sample: *c*, which has the smallest amplitude parameters (R_a, R_q) and also the highest skewness value. It has the smallest granule size in the thin film surface and, consequently, it has the highest surface area to enhance the efficiency (η % = 82.39%). The high negative value (R_{sk} = − 0.889) of skewness demonstrates that it has more valleys than peaks and asymmetrical distribution of particles which have collectively benefited to improve the surface area. The minimum efficiency (η % = 39.96) is shown by sample *g* which has the highest amplitude parameters (R_a = 111 nm, R_q = 137 nm) and relatively low skewness (R_{sk} = 0.308). Samples *e* and *f* are almost similar as far as the HPD efficiency is concerned where η % are 57.63 and 59.91%, respectively.

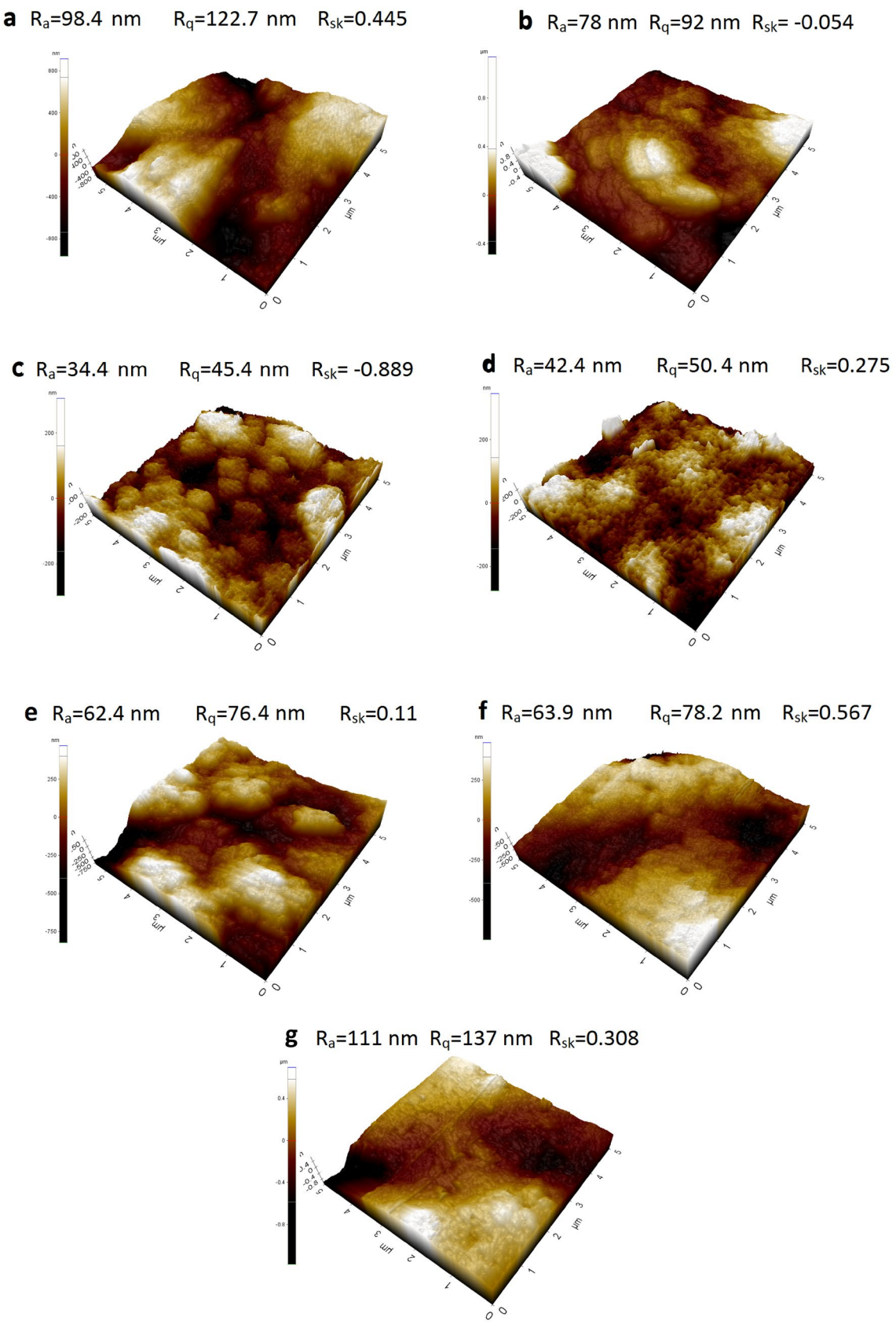

Fig. 6 Three-dimensional AFM images of N-TiO_2 thin film series

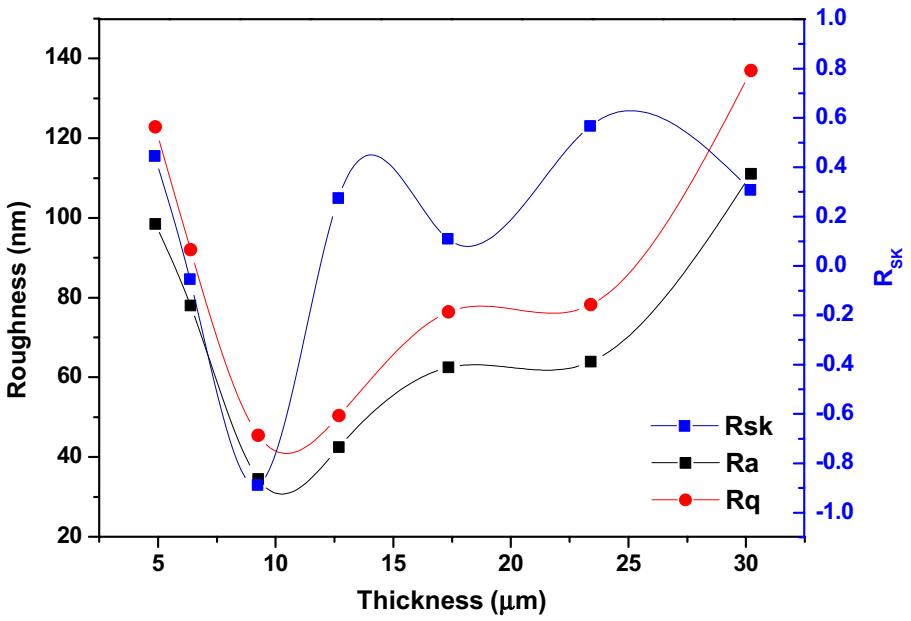

Fig. 7 Effect of the amplitude parameters (R_a and R_q) and skewness (R_{sk}) to the thin film series

Conclusion

We have investigated HPD reaction of toluene by visible light irradiated N-TiO_2 thin films. When TiO_2 nanoparticles doped with nitrogen, their band gap gets significantly decreased and TiO_2 has become visible light responsive. N-TiO_2 thin films were prepared and used to degrade indoor pollutants, namely $C_6H_5CH_3$, in static air condition. N-doped TiO_2 semiconductor thin films have been shown the higher $C_6H_5CH_3$ degradation rate. N-TiO_2 has high HPD efficiency when compared with P25 standard nanophotocatalyst. The effects of the HPD efficiency of toluene by N-TiO_2 on amount or mass and the thickness of the thin film have been examined and found that the efficiency is first increased when the thickness is increased and then it is decreased. The optimum thickness gives the highest surface area and penetration of light into the film. When the thickness is further increased, agglomeration results in decreasing surface area and preventing light penetration into the film. It was also found that toluene in static air degrades with various efficiencies when the films have multiple roughness. The AFM study reveals that there are some important factors that affect the toluene degradation efficiency. We found that when nanoparticles get smaller in the nanoscopic range, they show improvement of HPD efficiency due to the increment of surface area but the average roughness and other factors such as skewness (R_{sk}) are also important. The asymmetrical distribution of nanoparticles in thin films affects the nanoroughness of the coatings and layers.

Acknowledgements We would like to thank Ms. Nadeeka Tissera for her contribution in AFM and other studies.

References

1. De Silva, R.T., Mantilaka, M.M.M.G.P.G., Goh, K.L., Ratnayake, S.P., Amaratunga, G.A.J., Nalin de Silva, K.M.: Photocatalytic activity of electrospun MgO nanofibres: synthesis, characterization and applications. Mater. Res. Bull. **99**, 204–210 (2018)
2. Carp, O., Huisman, C.L., Reller, A.: Photoinduced reactivity of titanium dioxide. Prog. Solid State Chem. **32**, 33–177 (2004)
3. Hashimoto, K., Irie, H., Fujishima, A.: TiO_2 photocatalysis: a historical overview and future prospects. Jpn. J. Appl. Phys. **44**(12), 8269–8285 (2005)
4. Zhang, P., Tian, J., Xu, R., Ma, G.: Hydrophilicity, photocatalytic activity and stability of tetraethyl orthosilicate modified TiO_2 film on glazed ceramic surface. Appl. Surf. Sci. **266**, 141–147 (2013)
5. Bae, D.S., Han, K.S., Choi, S.H.: Preparation and thermal stability of doped TiO_2 composite membranes by the sol–gel process. Solid State Ionics **109**, 239–245 (1998)
6. Rzigalinski, B.A., Strobl, J.S.: Cadmium-containing nanoparticles: perspectives on pharmacology and toxicology of quantum dots. Toxicol. Appl. Pharmacol. **238**, 280–288 (2009)
7. Mills, A., Le Hunte, S.: An overview of semiconductor photocatalysis. J. Photochem. Photobiol. A **108**, 1–35 (1997)
8. Park, J.H., Kang, S.J., Na, S.I., Lee, H.H., Kim, S.W., Hosono, H., Kim, H.K.: Indium-free, acid-resistant anatase Nb-doped TiO_2 electrodes activated by rapid-thermal annealing for cost-effective organic photovoltaics. Sol. Energy Mater. Sol. Cells **95**, 2178–2185 (2011)
9. Yu, H., Zhang, S., Zhao, H., Will, G., Liu, P.: An efficient and low-cost TiO_2 compact layer for performance improvement of

dye-sensitized solar cells. Electrochim. Acta **54**, 1319–1324 (2009)
10. Yin, S., Yamaki, H., Komatsu, M., Zhang, Q., Wang, J., Tang, Q., Saito, F., Sato, T.: Synthesis of visible-light reactive $TiO_{2-X}N_Y$ photocatalysts by mechanochemical doping. Solid State Sci. **7**, 1479–1485 (2005)
11. Chou, ChS, Huang, Y.H., Wu, P., Kuo, Y.T.: Chemical-photoelectricity diagrams by Ohm's law—a case study of Ni- doped TiO_2 solutions in dye-sensitized solar cells. Appl. Energy **118**, 12–21 (2014)
12. Tung Lin, Y., Huang Weng, Ch., Ying Chen, F.: Key operating parameters affecting photocatalytic activity of visible-light-induced C doped TiO_2 catalyst for ethylene oxidation. Chem. Eng. J. **248**, 175–183 (2014)
13. Tang, W., Chen, X., Xia, J., Gong, J., Zeng, X.: Preparation of a Fe-doped visible-light-response TiO_2 film electrode and its photoelectrocatalytic activity. Mater. Sci. Eng. B **187**, 39–45 (2014)
14. Morikawa, T., Ohwaki, T., Suzuki, K., Moribe, S., Tero-Kubota, S.: Visible-light-induced photocatalytic oxidation of carboxylic acids and aldehydes over N-doped TiO_2 loaded with Fe, Cu or Pt. Appl. Catal. B **83**, 56–62 (2008)
15. Zhang, H., Yang, Z., Zhang, X., Mao, N.: Photocatalytic effects of wool fibers modified with solely TiO_2 nanoparticles and N-doped TiO_2 nanoparticles by using hydrothermal method. Chem. Eng. J. **254**, 106–114 (2014)
16. Ferrari-Lima, A.M., de Souza, R.P., Mendes, S.S., Marques, R.G., Gimenes, M.L., Fernandes-Machado, R.C.: Photodegradation of benzene, toluene and xylenes under visible light applying N-doped mixed TiO_2 and ZnO catalysts. Catal. Today **241**, 40–46 (2014)
17. Wang, Ch., Qian, HuQ, Quan Huang, J., Hua Deng, Z., Ling Shi, H., Wu, L., Guang Liu, Z., Ge Cao, Y.: Effective water splitting using N-doped TiO_2 films: role of preferred orientation on hydrogen production. Int. J. Hydrog. Energy **39**, 1967–1971 (2014)
18. Huang, Y., Wei, Y., Wu, J., Guo, Ch., Wang, M., Yin, S., Sato, T.: Low temperature synthesis and photocatalytic properties of highly oriented $ZnO/TiO_{2-x}N_y$ coupled photocatalysts. Appl. Catal. B **123**(124), 9–17 (2012)
19. De Silva, R.T., Mantilaka, M.M.M.G.P.G., Ratnayake, S.P., Amaratunga, G.A.J., de Silva, K.M.N.: Nano-MgO reinforced chitosan nanocomposites for high performance packaging applications with improved mechanical, thermal and barrier properties. Carbohyd. Polym. **157**, 739–747 (2017)
20. Wijesinghe, W.P.S.L., Mantilaka, M.M.M.G.P.G., Chathuranga Senarathna, K.G., Herath, H.M.T.U., Premachandra, T.N., Ranasinghe, C.S.K., Rajapakse, R.P.V.J., Rajapakse, R.M.G., Edirisinghe, Mohan, Mahalingam, S., Bandara, I.M.C.C.D., Singh, Sanjleena: Preparation of bone-implants by coating hydroxyapatite nanoparticles on self-formed titanium dioxide thin-layers on titanium metal surfaces. Mater. Sci. Eng. C **63**, 172–184 (2016)
21. Wijesinghe, W.P.S.L., Mantilaka, M.M.M.G.P.G., Rajapakse, R.M.G., Pitawala, H.M.T.G.A., Premachandra, T.N., Herath, H.M.T.U., Rajapakse, R.P.V.J.: Urea-assisted synthesis of hydroxyapatite nanorods from naturally occurring impure apatite rocks for biomedical applications. RSC Adv. **7**, 24806–24812 (2017)
22. Wu, D., Long, M.: Realizing visible-light-induced self-cleaning property of cotton through coating N-TiO_2 film and loading AgI particles. ACS Appl. Mater. Interfaces **3**, 4770–4774 (2011)
23. Li, C.Y., Li, X.P., Ma, Y.T., Wang, Z.P., Zhou, W.X., Lin, Y., Feng, S.J., Xiao, X.R.: A novel nanocrystalline TiO_2 thin film electrodes prepared at low temperature. Chin. Chem. Lett. **16**(7), 967–970 (2005)
24. Özdal, T., Hames, Y., Aslan, E.: A comparative study on TiO_2 doped hybrid solar cells. Appl. Surf. Sci. **258**, 5259–5264 (2012)
25. Webb, H.K., Truong, V.K., Hasan, J., Fluke, C., Crawford, R.J., Ivanova, E.P.: Roughness parameters for standard description of surface nanoarchitecture. Scanning **34**, 257–263 (2012)
26. Girginov, Ch., Stefchev, P., Vitanov, P., Hr, Dikov: Silver doped TiO_2 photocatalyst for methyl orange degradation. J. Eng. Sci. Technol. Rev. **5**(4), 14–17 (2012)
27. Kim, S.B., Hwang, H.T., Hong, S.C.: Photocatalytic degradation of volatile organic compounds at the gas–solid interface of a TiO_2 photocatalyst. Chemosphere **48**, 437–444 (2002)
28. Fasakin, O., Adebola Eleruja, M., Oluwole Akinwunmi, O., Olofinjana, B., Ajenifuja, E., Ajayi, E.O.B.: Synthesis and characterization of metal organic chemical vapour deposited copper titanium oxide (Cu–Ti–O) thin films from single solid source precursor. J. Mod. Phys. **4**, 1–6 (2013)
29. Lynch, J., Giannini, C., Cooper, J.K., Loiudice, A., Sharp, I.D., Buonsanti, R.: Substitutional or interstitial site-selective nitrogen doping in TiO_2 nanostructures. J. Phys. Chem. C **119**(13), 7443–7452 (2015)
30. Klanjšek Gunde, M., Kožar Logar, J., Crnjak Orel, Z., Orel, B.: Application of the Kubelka–Munk theory to thickness-dependent diffuse reflectance of black paints in the Mid-IR. Appl. Spectrosc. **49**, 623–629 (1995)